Jour. Korean Inst. Mining Geol.
Vol. 22, No. 4, p. 371-379, 1989

Temperature–Pressure Estimation of Metasediments in Seosan Area.

Yungoo Song,* Hi–Soo Moon*, and Han Yeang Lee**

Abstract : Peak or near–peak metamorphic temperatures and pressures for Seosan area could be estimated from major element method. Temperatures calculated from garnet–biotite geothermoneter(Ferry and Spear, 1978 ; Ganguly and Saxena, 1984) are 620±40℃ and 520±20℃ for Seosan and Daesan Formation respectively. Presures derived from garnet–plagiclase–Al_2SiO_5–quartz geobarometer(Newton and Haselton, 1981 ; Ganguly and Saxena, 1984)suggest 5–6kb for both of Seosan and Daesan Formation. These results suggest that under isobar ic, Seosan Formation underwent relatively high temperature metamorphism compared with Daesan Formation.
Chemical zonations of garnet for major elements such as Fe, Mg, and Mn in Seosan and Dasan Formation show different patterns each other probably caused by different thermal history.

INTRODUCTION

One goal of the metamophic petrology is to estimate the pressure–temperature conditions during metamorphic events. Experimental study on the various mineral equilibria in the past two decades enables us to determine the metamorphic conditions much more precisely.

In this study, geothermometer and geobarometer were used to estimate the metamorphic conditions in Seosan area. Precambrian metasediments in this area, Seosan Group, have mineral assemblages which can be applicable to the using of a certain geothermobarometer.

The primary purpose of this research is to evaluate an accurate temperature and pressure of Seosan and Daesan Formation in this area and this result is incorporated into a comparison which can recognize different metamorphic condition in each Formation.

GEOLOGICAL SETTING

Precambrian metasediments, Seosan Group, is divided into Seosan and Daesan Formation(Na et al., 1982a). Seosan Formation is composed of mica scist, biotite gneiss, banded gneiss, and iron–bearing interbedded quartzite and the grade of metamorphism varied from sillimanite zone to granet zone to the westward. Daesan Formation mostly consists of biotite gneiss and interbedded quartzite and shows unconformable relationship with Seosan Formation. This Formation is folded into synclinal fold with axis trending NE–SW and the grade of metamorphism is mainly staurolite–kyanite zone. In the western portion of the study area, Seosan Group is intruded by Precambrian granite gneiss. Age–unknown low–grade metasediment, Taean Formation, overlies uncomformably on these Precambrian rocks in the central portion of this area. Later, metasediments and granite gneiss are intruded by porphyritic syenite, deformed granite, and biotite granite. The simplified geological map of Seosan area is shown in Fig. 1.

* Department of Geology, Yonsei University, 134 Sinchondong, Seoul 120–749, Korea.
** Korea Institute of Energy and Resources, 71–2, Chang–Dong, Yuseong–Ku, Daejeon, 302–343, Korea.

ANALYTICAL TECHNIQUE

Approximately 150 samples of metasediments were collected ; sampling locations are marked in Fig. 1. Mineral assemblages were precisely observed under microscope and selected for the best result of analysis. Compositions of minerals were analyzed by using automated JCXA–Electron Microprobe in Yonsei University and data were reduced by Bence and Albee correction method(1968). Natural minerals were used for the standard materials ; albite for Si and Na, almandine for Al and Fe, olivine for Mg, rhodonite for Mn, rutile for Ti, diopside for Ca, and sanidine for K.

MINERAL ASSEMBLAGES

All samples of metasediments from the study area contain quartz and biotite, which have va-

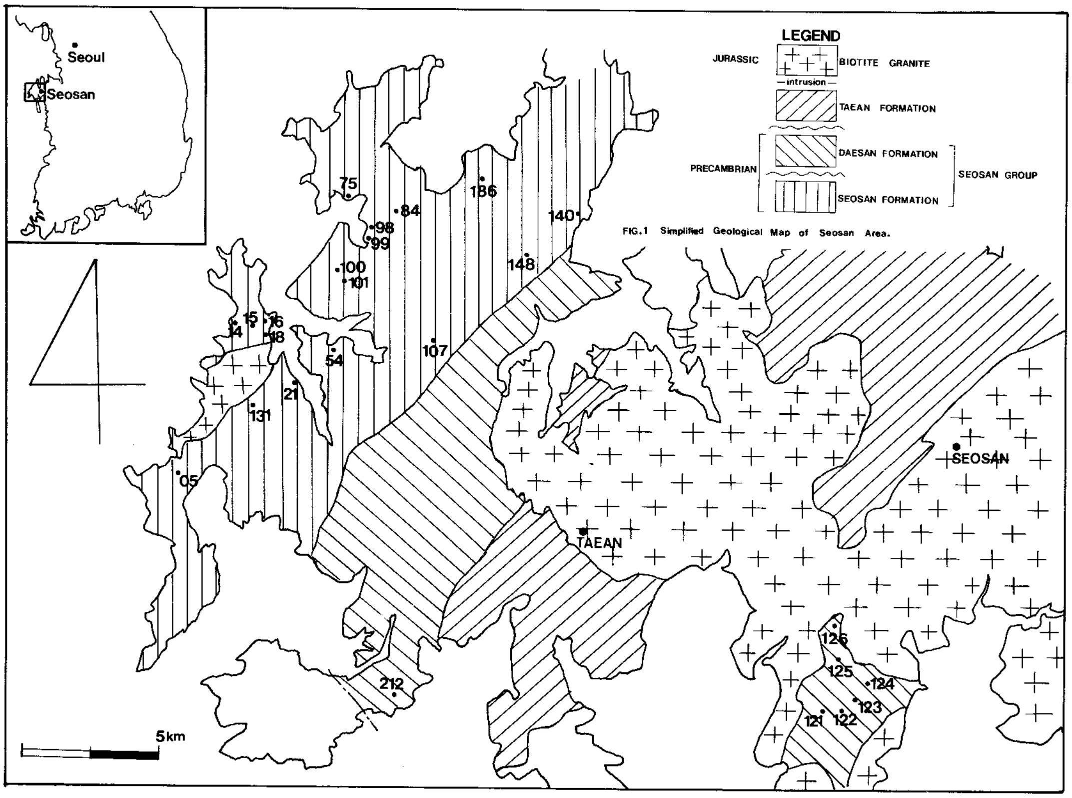

Fig. 1. Simplified geological map of Seosan area.

rious combinations of muscovite, plagioclase, garnet, sillimanite, staurolite, kyanite, cordierite, andalusite, and ilmenite. Samples of Seosan Formation are characterized by sillimanite–garnet assemblages, whereas those of Daesan Formation are characterized by staurolite–kyanite assemblages. In Seosan Formation, mineral assemblages are transitionally varied from sillimanite zone, through sillimanite–garnet zone, to garnet zone to the westward. Following assemblages are recognized ;

quartz–biotite–muscovite–sillimanite–plagioclase–ilmenite

quartz–biotite–muscovite–sillimanite–plagioclase–garnet– ilmenite

quartz–biotite–muscovite–plagioclase–garnet–ilmenite

In Daesan Formation, garnet, biotite, plagioclase, muscovite, in partially, cordierite and sillimanite are recognized.

Following assemblages are recognized ;

quartz–biotite–muscovite–garnet–plagioclase–ilmenite $\pm$sillimanite

quartz–biotite–muscovite–garnet–plagioclase–cordierite–ilmenite $\pm$ sillimanite

quartz–biotite–muscovite–garnet–plagioclase–kyanite– staurolite–ilmenite $\pm$cordierite

Representative polarizing microscopic photographs of these Formations are presented in Fig. 2.

MINERAL CHEMISTRY

Mineral assemblages of Seosan and Daesan Formation were discussed in earlier. Results of the microprobe analysis for biotite, garnet, and plagioclase are presented in Table 1, 2, and 3.

Biotite

As is the case with all metamorphic biotite, octahedral vacancies are common. A plot of Σ cation(VI) against Ti(Fig. 3–A) reveals that for the biotites coexisting with ilmenite in Seosan area, the vacancies are mainly associated with Ti content. Plots of Al(VI) against Ti and Mg/Fe against Ti(Fig. 3–B, C) reveal that content of Ti decreases with increasing of Al(VI) and Mg/Fe ratio. Guidotti et al.(1977) pointed that substitutions of the Ti, Si. and Al(IV) are exactly those required to achieve a stable state between the tetrahedral and octahedral sites, and thus minimize the amount of tetrahedral rotation otherwise required by high ratio of Mg/Fe in biotite. Decrease of Ti in the octahedral site

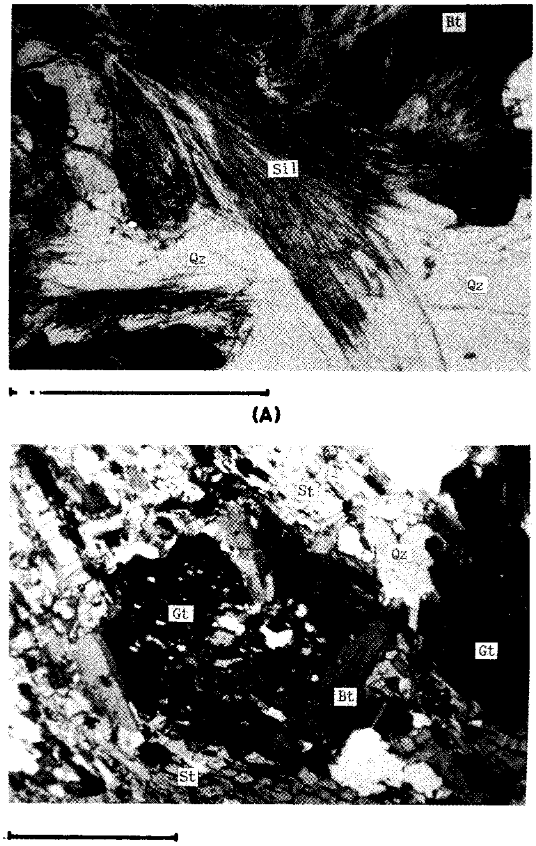

Fig. 2. Representative polarizing microscopic photograph of Seosan Group. Typically fibrous sillimanite in Seosan Formation ; A and coexisting biotite, garnet, and staurolite in Daesan Formation ; B. (Scale bar = 1mm)

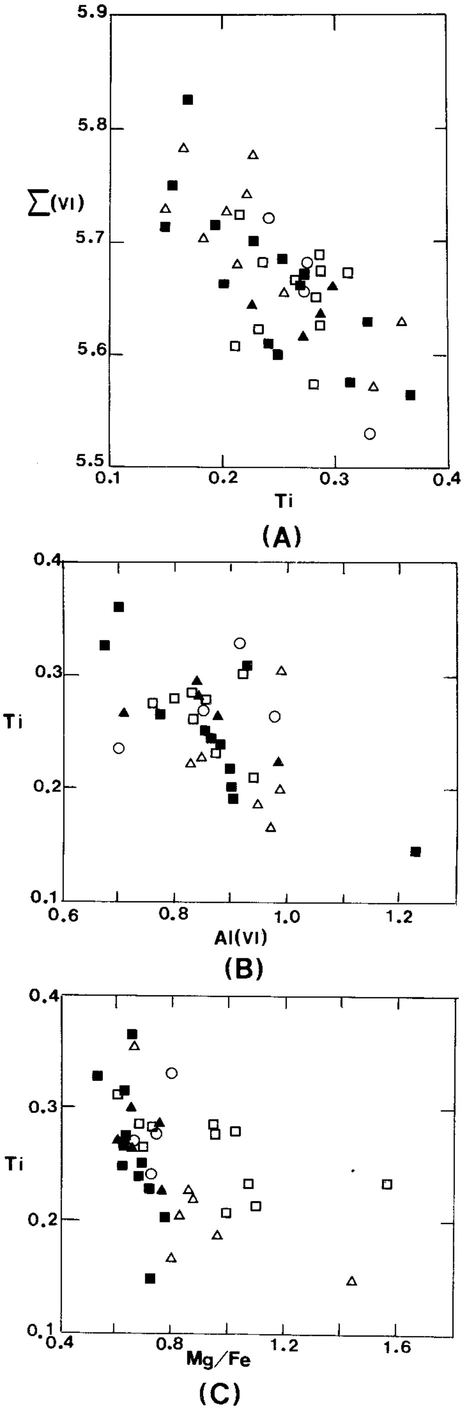

Fig. 3. Plot of Σcation(VI) vs. Ti in ions per 22–oxygen formulae unit for biotites ; A, Ti vs. Al(VI) ; B, and Ti vs. Mg/Fe ; C. Open circle : sil–bio–mus assem., solid triangle : sil–ga–bio–mus assem., solid rectangular : ga–bio assem.,open rectangular : bio–mus assem., and open triangle : st–ky–ga–bio–mus assem.

should also contribute to a decrease of rotation and lead to a decrease of Al(IV)(i.e.,increase of Si) for a charge balance. Therefore, it is revealed that the above chemical characteristics of biotites in this area are mainly dependent upon aspects of structural factor and a charge balance. Furthermore, the substitution of Al and Ti would affect the distribution of major elements such as Fe and Mg. The chemical zonation from core to rim composition is poor for most of biotites.

Garnet

Most garnets are zoned continuously from core to rim. Compositonal profiles of Mg, Fe, and Mn measured with an automatic scanning electron microprobe indicate that the aspect of zoning in Seosan Formation is incompatible with that of Daesan Formation(Fig. 4). The factors

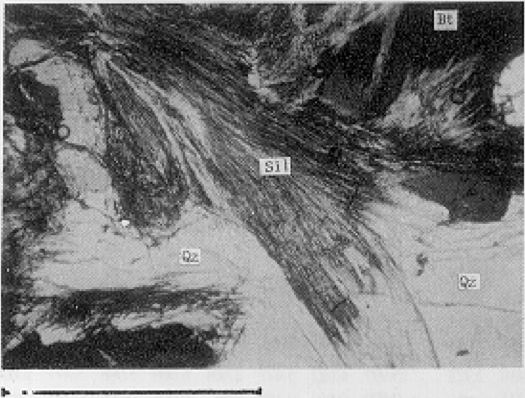

(A)

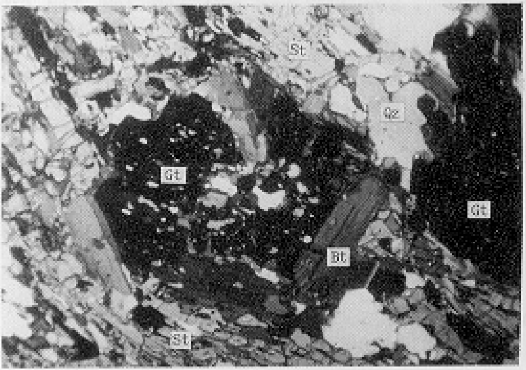

Table 1. Electron microprobe analyses for representative garnet, biotite, and plagioclase.

Sample	Seosan Formation											Daesan Formation							
	Y18			Y14				Y16				Y121a				$Y121_b$			
				Gt				Gt				Gt				Gt			
No.	Gt	Bt	Pl	(rim)	(core)	Bt	Pl	(rim)	(core)	Bt	Pl	(rim)	(core)	Bt	Pl	(rim)	(core)	Bt	Pl
SiO_2	37.05	33.87	60.02	36.63	37.40	34.35	61.63	37.17	36.90	34.31	60.92	37.38	37.76	35.81	58.74	37.36	37.13	35.81	58.74
TiO_2	0.01	2.51	—	—	—	2.09	—	—	0.01	2.03	—	0.03	0.08	1.61	—	0.01	0.04	1.61	—
Al_2O_3	20.89	19.24	24.60	20.79	21.02	19.08	23.70	21.18	21.05	18.75	24.16	21.18	21.11	19.44	26.34	21.14	21.00	19.44	26.34
FeO	34.16	20.58	0.06	33.06	32.70	20.71	0.04	32.09	33.16	20.04	0.14	33.47	29.69	18.02	0.06	34.05	29.85	18.02	0.06
MnO	3.95	0.11	—	5.32	4.67	0.15	—	6.50	4.66	0.18	—	0.83	5.68	0.09	—	0.15	5.64	0.09	—
MgO	2.22	7.49	—	2.19	2.54	7.17	—	1.82	2.35	7.69	—	2.69	1.69	9.73	—	3.14	1.75	9.73	—
CaO	1.60	0.04	6.29	1.04	1.14	0.06	5.40	1.22	1.31	0.03	5.78	4.34	5.01	0.10	8.66	3.77	4.68	0.10	8.66
Na_2O	0.01	0.27	7.90	0.02	—	0.23	8.48	0.01	—	0.20	8.29	—	—	0.27	6.94	—	—	0.27	6.94
K_2O	0.01	8.84	0.21	0.02	—	9.43	0.09	—	—	9.58	0.14	0.01	0.01	8.48	0.06	0.01	—	8.48	0.06
Total	99.90	92.95	99.08	99.07	99.47	93.27	99.34	99.99	99.44	92.81	99.43	99.93	101.03	93.55	100.80	99.63	100.09	93.55	100.80
Si	6.008	5.325	2.696	5.998	6.054	5.397	2.750	6.021	6.000	5.410	2.723	5.997	6.022	5.477	2.608	6.000	5.988	5.477	2.608
Ti	0.001	0.297	—	—	—	0.247	—	—	0.001	0.241	—	0.004	0.010	0.185	—	0.001	0.005	0.185	—
Al	3.992	3.565	1.302	4.012	4.010	3.533	1.246	4.044	4.034	3.484	1.273	4.005	3.968	3.504	1.378	4.002	3.992	3.504	1.378
Fe	4.632	2.706	0.002	4.527	4.427	2.721	0.001	4.347	4.509	2.642	0.005	4.490	3.960	2.305	0.002	4.573	4.026	2.305	0.002
Mn	0.543	0.015	—	0.738	0.640	0.020	–	0.892	0.642	0.024	–	0.113	0.767	0.012	—	0.020	0.770	0.012	–
Mg	0.537	1.755	—	0.534	0.613	1.679	—	0.439	0.570	1.807	–	0.643	0.402	2.218	—	0.752	0.421	2.218	—
Ca	0.278	0.007	0.303	0.182	0.198	0.010	0.258	0.212	0.228	0.005	0.277	0.746	0.856	0.016	0.412	0.649	0.809	0.016	0.412
Na	0.003	0.082	0.688	0.006	—	0.070	0.734	0.003	–	0.061	0.719	—	—	0.080	0.597	—	—	0.080	0.597
K	0.002	1.773	0.012	0.004	—	1.890	0.005	—	—	1.927	0.008	0.002	0.002	1.655	0.003	0.002	—	1.655	0.003
O	24.000	22.000	8.000	24.000	24.000	22.000	8.000	24.000	24.000	22.000	8.000	24.000	24.000	22.000	8.000	24.000	24.000	22.000	8.000

* Gt : Garent
Bt : Biotite
Pl : Plagioclase

Table 2. Structural formulae for garnet, biotite, and plagioclase.

	Sample No.		Garnet X_{Mg}	X_{Fe}	X_{Ca}	X_{Mn}	Biotite X_{Al}^{VI}	X_{Ti}	X_{Mg}	X_{Fe}	X_{Mn}	Plagioclase X_{Ca}	X_{Na}
	Y05	(R)	0.485	4.253	0.383	0.862	0.979	0.201	1.940	2.521	0.020	–	–
		(C)	0.557	4.407	0.402	0.568	0.979	0.201	1.940	2.521	0.020	–	–
	Y14	(R)	0.534	4.527	0.182	0.738	0.931	0.247	1.680	2.721	0.020	0.258	0.734
		(C)	0.613	4.427	0.198	0.640	0.931	0.247	1.680	2.721	0.020	0.258	0.734
	Y15		0.537	4.538	0.276	0.566	0.995	0.192	1.658	2.850	0.020	0.294	0.698
	Y16	(R)	0.439	4.347	0.212	0.892	0.894	0.241	1.808	2.642	0.024	0.277	0.719
		(C)	0.570	4.509	0.228	0.642	0.894	0.241	1.808	2.642	0.024	0.277	0.719
	Y18		0.537	4.632	0.278	0.542	0.890	0.297	1.755	2.705	0.015	0.303	0.688
Seosan	Y21		0.718	4.520	0.185	0.576	0.914	0.285	1.895	2.520	0.021	0.255	0.751
Formation	Y54		0.544	4.538	0.365	0.476	0.970	0.252	1.820	2.634	0.012	–	–
	Y84		0.458	4.621	0.236	0.649	0.756	0.327	1.566	2.960	0.021	0.261	0.721
	Y98		0.522	4.394	0.219	0.829	0.944	0.228	1.881	2.636	0.013	0.239	0.747
	Y99		0.478	4.469	0.254	0.765	0.954	0.312	1.635	2.655	0.019	–	–
	Y100		0.622	4.748	0.172	0.356	0.875	0.269	1.757	2.739	0.029	–	–
	Y107		0.507	4.131	0.259	1.117	1.034	0.225	1.877	2.483	0.027	–	–
	Y140	(R)	0.546	4.270	0.236	0.899	1.083	0.268	1.640	2.649	0.022	–	–
		(C)	0.569	4.399	0.179	0.816	1.083	0.268	1.640	2.649	0.022	–	–
	Y148		0.551	4.168	0.247	1.032	0.979	0.266	1.776	2.731	0.031	0.281	0.719
	Y186		0.585	4.469	0.177	0.725	0.919	0.270	1.644	2.763	0.020	0.217	0.809
	Y121a	(R)	0.643	4.490	0.746	0.113	0.982	0.185	2.219	2.305	0.012	0.412	0.597
		(C)	0.402	3.960	0.856	0.767	0.982	0.185	2.219	2.305	0.012	0.412	0.597
Daesan	Y121b	(R)	0.752	4.573	0.649	0.020	0.982	0.185	2.219	2.305	0.012	0.412	0.597
Formation		(C)	0.421	4.026	0.809	0.770	0.982	0.185	2.219	2.305	0.012	0.412	0.597
	Y124	(R)	0.544	4.321	0.797	0.397	0.888	0.220	2.147	2.464	0.022	0.508	0.491
		(C)	0.439	3.900	0.689	0.931	0.888	0.220	2.147	2.464	0.022	0.508	0.491

Table 3. Chemical analyses of ferrous iron oxide and structural formulae on the basis of 22 oxygens for bioties.

	Sample No.	Fe_2O_3	FeO	X^{VI}_{Al}	X_{Ti}	X_{Mg}	$X_{Fe^{3+}}$	$X_{Fe^{2+}}$	X_{Mn}
Seosan Formation	Y05	3.36	16.51	0.900	0.199	1.923	0.387	2.113	0.019
	Y14	2.72	18.26	0.867	0.245	1.667	0.319	2.382	0.020
	Y15	4.07	18.22	0.898	0.190	1.640	0.472	2.348	0.020
	Y16	0.62	19.48	0.880	0.240	1.804	0.073	2.564	0.024
	Y18	2.16	18.64	0.838	0.295	1.745	0.254	2.436	0.015
	Y21	3.05	16.89	0.842	0.283	1.879	0.349	2.151	0.021
	Y54	4.92	16.06	0.856	0.249	1.796	0.562	2.038	0.012
	Y84	3.41	19.37	0.676	0.324	1.551	0.401	2.531	0.021
	Y98	2.08	18.60	0.894	0.227	1.870	0.240	2.383	0.013
	Y99	1.01	19.85	0.931	0.311	1.630	0.116	3.532	0.019
	Y100	4.49	17.33	0.773	0.265	1.736	0.512	3.195	0.028
	Y107	2.16	17.85	0.984	0.223	1.866	0.243	2.227	0.027
	Y134	1.94	16.61	0.914	0.327	1.846	0.223	2.122	0.021
	Y148	4.45	17.25	0.874	0.263	1.755	0.509	2.192	0.031
	Y184	3.18	16.93	0.851	0.271	1.868	0.367	2.174	0.035
	Y188	3.07	17.79	0.977	0.267	1.697	0.347	2.231	0.028
Daesan Formation	Y121	1.21	16.93	0.953	0.185	2.211	0.139	2.159	0.012
	Y122	0.92	18.25	0.991	0.203	2.027	0.107	2.354	0.014
	Y123	2.43	17.07	0.850	0.227	2.125	0.279	2.176	0.027
	Y124	2.42	17.15	0.833	0.219	2.133	0.276	2.172	0.022
	Y125	1.78	18.45	0.964	0.165	2.007	0.204	2.356	0.022
	Y126	3.10	17.06	0.989	0.353	1.649	0.354	2.163	0.013

of crystalization rate, inter–intra diffusion rate, bulk composition, and temperature can affect the zoning profile of garnet. In Seosan Formation, zoning profiles show typical patterns of garnet in amphibolite facies rocks and homogeneous compositions of Fe and Mn over a large area of the core reflect relatively higher metamorphic temperature, whereas in Daesan Formation, the chemical zoning is reversed compared to those of Seosan Formation. Slight increase of Mn content near the rim in Seosan Formation suggests that the garnet underwent late–stage resorption or diffusional zoning probably caused by the different rate between crystallization and inter–diffusion, and in Daesan Formation a continuous decrease in Mn from core to rim indicates that the garnet was gradually grown with decreasing of temperature(Tracy, 1982).

Plagioclase

Plagioclase is commonly observed in the Seosan Group. It is characteristically revealed that An components are different between two Formations ; An_{20-30} and An_{35-50} for Seosan and Daesan Formation respectively. Different contents of An in plagioclase for Seosan and Daesan Formation suggest different metamorphic conditions such as temperature, P_{H_2O}, bulk composition, and secondary resorption.

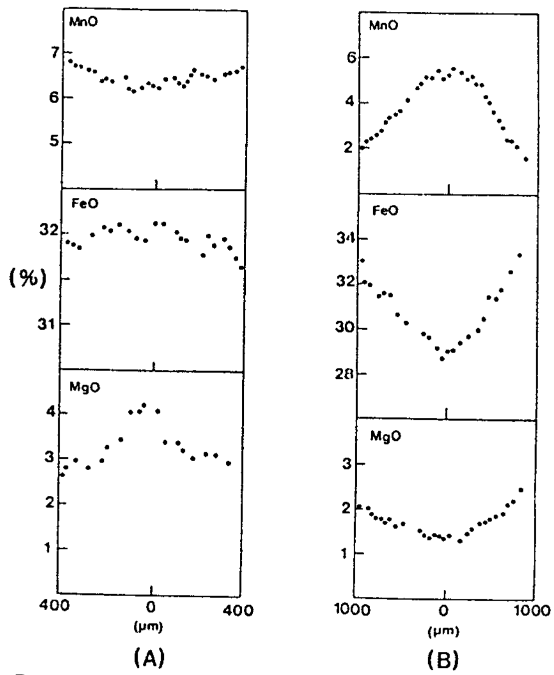

Fig. 4. Compositional profiles of Mg, Fe, and Mn measured with an electron microprobe in garnet from Seosan and Daesan Formation. A ; Seosan Formation, B ; Daesan Formation.

Other Minerals

The octahedral occupancy of all muscovites is remarkably constant averaging 4.051±0.026 based on 22 oxygens. This suggests that any substitutions involving octahedral vacancies must be nearly constant in amount for all muscovites and there is a limited and constant amount of trioctahedral substitution. Compositions of muscovites in the interlayer site contents reveal the remarkable differences between Seosan and Daesan Formation.

Staurolite is observed in Daesan Formation and is elongated into the direction of schistosity. Each element is remarkably constant on a 46-oxygen basis. Mn and Ti content are constantly low and values of Fe/(Fe+Mg) for the staurolite range from 0.82 to 0.83. Staurolite shows no chemical zoning.

Three phases of aluminum silicate are observed in Seosan Group. Sillimanite is commonly observed in Seosan Formation, but in part observed in Daesan Formation. Sillimanite appearance in Daesan Formation could be explained by the progressive temperature change caused by late intrusion of Juassic granite. Kyanite is recognized only in Daesan Formation. Only small amounts of andalusite appeared in Seosan Formation may be responsible for the retrogressive temperature change.

Cordierite is recognized only in Daesan Formation. Composition of each element is nearly constant on a 28-oxygen basis and values of Fe/(Fe+Mg) are average of 0.38.

METAMORPHIC TEMPERATURE-PRESSURE ESTIMATION

Garnet-Biotite Geothermometer

The calibration of Fe-Mg distribution between garnet and biotite has been made by Thompson(1976), Goldman and Albee(1977), Ferry and Spear(1978), Ganguly and Saxena(1984), and Indares and Martignole(1985). Thompson's empirical calibration is based largely on comparison of natural assemblages with experimental phase equilibria. Goldman and Albee(1977) calibrated on temperatures through quartz-magnetite geothermometer based on the exchange of oxygen isotope. The Ferry and Spear's calibration(1978) is based on experiments in the purely Fe-Mg binary system. Ganguly and Saxena(1984) introduced non-ideality term using their garnet solid solution model and modified Ferry and Spear's result. Indares and Martignole(1985) considered the effect of Ti and Al in biotite on the Fe-Mg distribution between these two minerals.

Table 4 shows temperatures derived from geothermometers of Ferry and Spear(1978),

Table. 4. Equilibrium temperatures calculated from gt-bt geothermometer.

	Sample No.		Temperature(℃) at 6kb (A)		(B)	
			F-S	G-S	F-S	G-S
Seosan Formation	Y14	(R)	608	637	565	592
		(C)	669	679	620	629
	Y16	(R)	524	570	516	562
		(C)	595	615	586	605
	Y18		584	609	551	575
	Y21		645	632	590	577
	Y84		600	645	551	593
	Y98		560	592	531	561
	Y99		574	616	560	601
	Y140	(R)	637	668	-	-
		(C)	641	665	-	-
	Y148		631	664	558	588
	Y186		662	681	-	-
Daesan Formation	Y121a	(R)	526	530	507	511
		(C)	435	492	420	477
	Y121b	(R)	569	548	548	528
		(C)	442	496	427	480
	Y124	(R)	517	547	484	512
		(C)	486	539	455	506

* F-S : Ferry and Spear(1978)
G-S : Ganguly and Saxena(1984)
(A) : All irons in biotite as ferrous
(B) : FeO after subtracting Fe_2O_3 from total Fe in biotite.

Ganguly and Saxena(1984), and Indares and Martignole(1985). The results of Ferry and Spear(1978) and Ganguly and Saxena(1984) are reasonably compatible. However Indares and Martignole's temperatures are lower than those of others by 40-70℃. In other literatures, the results of Indares and Martignole(1985) always indicate lower temperatures compared with those of independent methods. Fe component in biotite are considered as not only total Fe(column A) but FeO after subtracting Fe_2O_3 from total Fe(column B). Average temperatures for Seosan and Daesan Formation estimated from Ganguly and Saxena(1984) considering total iron as ferrous are about 620±40℃ and 520±20℃ respectively under reference pressure of 6kb. Rim compositions of coexisting biotite and garnet, which can reflect chemical equilibrium, are mainly concerned for this work. These estimates would be lowered by 30-50℃, provided considering Fe^{3+} in biotites($X_{Fe^{3+}}$ = 0.04-0.18). However, this result can not disturb seriously the previous estimation based on total irons in biotites since this lowered 30-50℃ is in the range of estimating errors. From the above result, metamorphic temperatures in Seosan Formation show higher temperatures by 100℃ compared with those in Daesan Formation.

Table. 5. Equilibrium temperatures and pressures calculated from gt–bt geothermometer and gt–pl–Al_2SiO_5–qz geobarometer.

	Sample No.		T(℃)	P(kb) N–H	T(℃)	P(kb) G–S
	Y14	(R)	634	4.7	637	5.3
		(C)	681	6.0	683	6.4
	Y16	(R)	564	3.7	567	4.7
Seosan		(C)	612	4.8	615	5.6
Formation	Y18		608	5.0	611	5.8
	Y21		629	4.7	631	5.3
	Y84		646	5.7	648	6.2
	Y98		590	5.0	593	5.8
	Y148		668	6.5	670	7.0
	Y186		685	6.7	686	6.8
	Y121a	(R)	529	5.2	533	6.1
		(C)	491	5.0	494	6.0
Daesan	Y121b	(R)	548	5.2	551	6.1
Formation		(C)	494	4.9	497	5.9
	Y124	(R)	547	5.5	549	6.2
		(C)	538	5.2	540	5.9

* Temperatures are calculated form gt–bt geothermometer of Ganguly and Saxena(1984)
N–H : Newton and Haselton(1981)
G–S ; Ganguly and Saxena(1984)

Garnet-Plagiocalse-Al_2SiO_5-Quartz Geobarometer

Pressure estimation from the reaction, 3 Anorthite = Grossular + $2Al_2SiO_5$ + Quartz, required an accurate activity data of garnet and plagioclase as a function of temperature, pressure, and composition. We have derived pressures using the methods of Newton and Haselton(1981) and Ganguly and Saxena(1984).

Table 5 shows pressures calculated from this geobarometer. Garnet–biotite temperatures calculated from Ganguly and Saxena(1984) were used in these calculations and all irons in biotites were assumed to be ferrous. Pressures calculated from Ganguly and Saxena(1984) tend to be higher than those estimated from Newton and Haselton(1981) by 0.5–0.8kb. The concentration of grossular in garnet analyzed by electron microprobe has been expressed by the atomic ratio of Ca/(Mg+Fe+Ca) for the simple calculation of activity terms in ternary system of garnet solid solution(Total iron is treated as ferrous). Estimations indicate that higher grossular component leads to higher pressure at constant temperature. In this area, metamorphic pressures combined with results of Ganguly and Saxena(1984) and Newton and Haselton(1981) are about 5–6kb for both of Seosan and Daesan Formation in spite of the difference in temperatures by about 100℃.

DISCUSSION

Metamorphic temperatures and pressures in Seosan area estimated from garnet–biotite geothermom eter and garnet-plagioclase–Al_2SiO_5–quartz geo barometer are summarized in Fig. 5. Temperatures

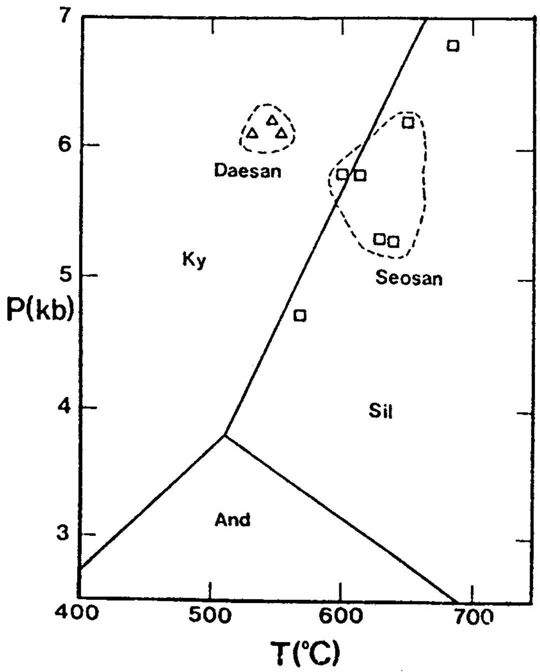

Fig. 5. Pressure–temperature diagram for Seosan and Daesan Formation. Open rectangulars and triangles indicate Seosan and Daesan Formation respectively calculated from Ganguly and Saxena(1984).

and pressures calculated from Ganguly and Saxena(1984) for Seosan and Daesan Formation are plotted in the stability field of sillimanite and kyanite respectively. These results are compatible with mineral assemblages observed in each sample and as discussed earlier, they represent reasonable agreement with temperatures and pressures of Ganguly and Saxena(1984) and Newton and Haselton(1981).

Calculated P–T conditions suggest that under isobaric, Seosan Formation experienced relatively high temperature metamorphism compared with Daesan Formation. Temperatures and pressures estimated from this work represent peak or near–peak temperature and pressure during metamorphic event since a blocking temperature of garnet is generally assumed to be above 500℃.

Chemical zonations of garnet in Seosan and

Daesan Formation show typical patterns of zoning compared with those described in other literatures ; zonation of garnet in Seosan Formation, which has homogeneous compositions over the wide area of the core, reflects high metamorphic temperature that can cause extensive intra-diffusion, whereas garnet in Daesan Formation has heterogeneous compositions over the core area, which can suggest lower metamorphic temperature compared with that of Seosan Formation. In the rim compositions of garnet, there are too many factors to interpret each pattern of zonation, so account for the zonation of the rim is not considered due to the lack of other data.

In this study, we merely suggest peak or near-peak metamorphic conditions for Seosan and Daesan Formation respectively and further studies are necessary to reconstruct the thermal history of these Formations in detail.

REFERENCES

Bence, A. E. and Albee, A. L.(1968) Empirical correction factors for the electron microanalysis of silicates and oxide. J. Geology, v. 76, p. 382–403.

Chang, T. W. and Lee, S. Y.(1982) Explanatory text of the geological map of Seosan and Mohang Sheets. K.I.E.R.

Cheney, J. T. and Guidotti, C. V.(1979) Muscovite–plagioclase equilibria in sillimanite+quartz-bearing metapelites, Puzzle Mountain area, Northwest Maine. Am. J. Science, v. 279, p. 411–434.

Dymek, R. F.(1983) Titanium, aluminum, and interlayer cation substitutions in biotite from high-grade gneisses, West Greenland. Am. Min., v. 68, p. 880–899.

Ferry, J. M.(1980) A comparative study of geothermometers and geobarometers in pelitic schists from south–central Maine. Am. Min., v. 65, p. 720–732.

Ferry, J. M. and Spear, F. S.(1978) Experimental calibration of the partitioning of Fe and Mg between biotite and garnet. Contr. Min. Petr., v. 66, p. 113–117.

Ganguly, J. and Saxena, S. K.(1984) Mixing properties of aluminosilicate garnets : constraints from natural and experimental data, and applications to geothermo–barometry. Am. Min., v. 69, p. 88–97.

Ghent, E. D., Robbins, D. B., and Stout, M. Z.(1979) Geothermometry, geobarometry, and fluid compositions of metamorphosed calc–silicates and pelites, Mica Creek, British Columbia. Am. Min., v. 64, p. 874–885.

Ghent, E. D. and Stout, M. Z.(1981) Geothermometry and geobarometry of plagioclase–biotite–garnet–muscovite assemblages. Cont. Min. Petr., v. 76, p. 92–97.

Goldman, D. S. and Albee, A. L.(1977) Correlation of Mg/Fe partitioning between garnet–biotite with O^{18}/O^{16} partitioning in between quartz and magnetite. Am. J. Science, v. 277, p. 750–761.

Green, N. L. and Usdansky, S. I.(1986) Toward a practical plagioclase–muscovite thermometer. Am. Min., v. 71, p. 1109–1117.

Guidotti, C. V., Cheney, J. T., and Guggenheim, S.(1977) Distribution of titanium between coexisiting muscovite and biotite in pelitic schists from northwestern Maine. Am. Min., v. 62, p. 438–448.

Hodges, K. V. and Spear, F. S.(1982) Geothermometry, geobarometry and the Al_2SiO_5 triple point at Mt. Moosilauke, New Hampshire. Am. Min., v. 67, p. 1118–1134.

Holdaway, M. J., Dutrow, B. L., and Hinton, R. W.(1988) Devonian and Carboniferous metamorphism in west–central Maine : The muscovite–almandine geobaromerter and the staurolite problem revisited. Am. Min., v. 73, p. 20–47.

Indares, A. and Martignole, J.(1985) Biotite–garnet geothermometry in the granulite facies : The influence of Ti and Al in biotite. Am. Min., v. 70, p. 272–278.

Na, K. C., Kim, H. S., and Lee, S. H.(1982a) Stratigraphy and Metamorphism of Seosan Group. J. Korean Inst. Mining Geol., v. 15, p. 33–39.

Na, K. C., Kim, H. S., Lee, D. J., and Lee, S. H.(1982b) Comparative studies between Chungju and Seosan Groups. J. Korean Inst. Mining Geol., v. 15, p. 177–188.

Newton, R. C. and Haselton, H. T.(1981) Thermodynamics of the garnet–plagioclase–Al_2SiO_5–quartz geobarometer. In Newton et al.(ed.) Thermodynamics of Minerals and Melts. New York, Spring–Verlag. p. 131–147.

Thompson, A. B.(1976) Mineral reactions in pelitic rocks : I. Prediction of P–T–X(Fe–Mg) phase relations. Am. J. Science, v. 276, p. 401–424.

Tracy, R. J.(1978) High grade metamorphic reactions and partial melting in pelitic schists, west–central Massachusetts. Am. J. Science, v. 278, p. 150–178.

————(1982) Compositional zoning and inclusions in metamorphic minerals. Min. Soc. of Am. Reviews in Mineralogy, v. 10, p. 355–397.

서산지역의 변성퇴적암류에 대한 온도—압력 추정

송 윤 구 · 문 희 수 · 이 한 영

요약 : 서산지역의 변성퇴적암류에 대한 변성온도 및 압력 조건이 공존하는 변성광물에 대한 분석결과로부터 측정될 수 있었다. 석류석과 흑운모 지온계(Ferry and Spear, 1978; Ganguly and Saxena, 1984)를 이용한 온도 측정 결과, 서산층에서는 620±40℃이며, 대산층에서는 520±20℃인 것으로 나타났다. 석류석—사장석—Al_2SiO_5—석영 지압계(Newton and Haselton, 1981; Ganguly and Saxena, 1984)을 이용한 압력 측정 결과, 두 층 모두 5—6kb로, 유사한 압력 조건을 보여주고 있다. 이같은 결과는 같은 압력 조건 아래에서 서산층이 대산층보다 상대적으로 높은 온도의 변성작용을 받았음을 제시해 준다.

서산층과 대산층에서 Fe, Mg, Mn 등 주원소에 대한 석류석의 chemical zonation은 서로 다른 양상을 보여 주는데, 아마도 두 층이 다른 열적 변성과정(thermal history)을 받아온 결과인 것같다.